um among the C_1- and C_2-species with atomic hydrogen. The correct prediction of the temperature and concentration profiles are a vital test of our ability to understand plasma chemistry at the boundary layer, specifically the dependence on gas-phase reactions and the contribution of surface reactions.

REFERENCES AND NOTES

1. R. L. Farrow and D. J. Rakestraw, *Science* **257**, 1894 (1992).
2. R. L. Abrams, J. F. Lam, R. C. Lind, D. G. Steel, P. F. Liao, in *Optical Phase Conjugation*, R. A. Fisher, Ed. (Academic Press, New York, 1983), p. 211.
3. The plasma is produced by a commercial, atmospheric-pressure radio frequency, inductively coupled, plasma torch. Typical feed-gas conditions (in liters per minute) are: Ar, 106.5; H_2, 12.0; and CH_4, 0.55. The net plasma enthalpy is about 7 kW leaving the nozzle exit, and the free-stream electron density is on the order of 10^{15} cm^{-3}. Substrates are held by a translation stage and positioned in the stagnation flow geometry of Fig. 1. A molybdenum substrate with surface temperature maintained near 1300 K is used for plasma conditions that promote diamond deposition. When the plasma is driven to higher temperatures and beyond diamond synthesis conditions, a water-cooled copper disk is substituted for the molybdenum substrate.
4. T. G. Owano, C. H. Kruger, M. A. Cappelli, *Mater. Res. Soc. Symp. Proc.* **190**, 131 (1991); M. A. Cappelli, T. G. Owano, C. H. Kruger, *J. Mater. Res.* **5**, 2326 (1990); T. G. Owano, C. H. Kruger, D. G. Goodwin, in preparation.
5. J. Pender and L. Hesslink, *Opt. Lett.* **10**, 264 (1985).
6. J. M. Ramsey and W. B. Whitten, *Anal. Chem.* **59**, 167 (1987).
7. P. Ewart, P. Snowdon, I. Magnusson, *Opt. Lett.* **14**, 563 (1989).
8. W. G. Tong, J. M. Andrews, Z. Wu, *Anal. Chem.* **59**, 896 (1987); J. M. Andrews and W. G. Tong, *Spectrochim. Acta Part B* **44**, 101 (1989); J. M. Andrews, K. M. Weed, W. G. Tong, *Appl. Spectrosc.* **45**, 697 (1991).
9. P. Ewart and S. V. O'Leary, *Opt. Lett.* **11**, 279 (1986); P. Ewart and M. Kaczmarek, *Appl. Opt.* **30**, 3996 (1991).
10. T. Dreier and D. J. Rakestraw, *Opt. Lett.* **15**, 72 (1990); *Appl. Phys. B* **50**, 479 (1990); D. J. Rakestraw, R. L. Farrow, T. Dreier, *Opt. Lett.* **15**, 709 (1990).
11. B. Yip, P. M. Danehy, R. K. Hanson, *Opt. Lett.* **17**, 751 (1992).
12. B. A. Mann, S. V. O'Leary, A. G. Astill, D. A. Greenhalgh, *Appl. Phys. B* **54**, 271 (1992).
13. S. Williams, D. S. Green, S. Sethuraman, R. N. Zare, *J. Am. Chem. Soc.* **114**, 9122 (1992).
14. D. A. Chen and W. G. Tong, *J. Anal. At. Spectrom.* **3**, 531 (1988); W. G. Tong and D. A. Chen, *Appl. Spectrosc.* **41**, 586 (1987).
15. D. G. Goodwin, *Appl. Phys. Lett.* **59**, 277 (1991); ______ and G. G. Gavillet, *J. Appl. Phys.* **68**, 6393 (1990).
16. S. J. Harris and D. G. Goodwin, *J. Phys. Chem.* **97**, 23 (1993).
17. S. J. Harris, *Appl. Phys. Lett.* **56**, 2298 (1990).
18. D.S.G. is a Natural Science and Engineering Research Council (Canada) postdoctoral fellow. S.W. is an Air Force Office of Scientific Research graduate scholar. This work was supported by several sources: C.H.K. acknowledges support from the Department of Energy under contract DE-FG03-88ER13957 and R.N.Z. from the Department of Energy under contract DE-FG03-92ER14304.

26 October 1992; accepted 23 December 1992

Cryptic Grain-Scale Heterogeneity of Oxygen Isotope Ratios in Metamorphic Magnetite

John W. Valley* and Colin M. Graham

Oxygen isotope ratios measured by ion microprobe in magnetite from granulite-facies marble of the Adirondack Mountains, New York, range from +2 to +11 per mil (standard mean ocean water) across a single grain that measures 3 millimeters by 5 millimeters. Low values are concentrated in irregular domains near the grain boundary but also occur in the grain's interior. In contrast, grains 1 millimeter in diameter that are from a second nearby sample show no significant heterogeneity, except within 10 micrometers of the grain boundary. These data, including large gradients of up to 9 per mil per 10 micrometers, provide important new constraints on the nature and origins of intragrain isotopic heterogeneity and on oxygen isotope thermometry. The differences between these magnetite grains result from contrasting mechanisms of isotope exchange with fluids after the peak of regional metamorphism. Volume diffusion of oxygen through the crystal structure of magnetite contributed to isotope exchange in the rims of small grains, but larger grains are crosscut by healed cracks that are not readily detected and that short-circuited diffusion.

The fractionation of oxygen isotopes between coexisting minerals should, in theory, provide an ideal means by which to determine the temperature of formation for many rocks (*1–5*). Appropriate mineral assemblages are plentiful, fractionation coefficients are well calibrated, temperature sensitivity is good, and there is no measurable pressure correction. However, the actual reliability of the results of stable isotope thermometry in igneous and metamorphic rocks is controversial (*1, 4, 6–11*).

Thermometers have often been thought to reset after mineral crystallization by exchange within and among minerals. Experimental data on oxygen self-diffusion in minerals have been used in models of retrograde exchange and, in some cases, in estimates of cooling rates (*7–10, 12*). The approximate agreement of two or more temperatures estimated from different mineral pairs in the same rock is often taken as proof that the estimate is accurate, but apparent agreement can arise in spite of retrogression.

Recent numerical modeling has shown that, because grain boundaries are zones of relatively rapid diffusion, there is not a simple blocking-temperature relation for diffusion [as in (*13*)]. In addition, closed-system exchange depends on modal proportions of all of the minerals in a rock as well as their mineral diffusivities, grain sizes, grain shapes, and cooling rates (*10*). Furthermore, oxygen diffusivity in some minerals is greatly enhanced by high water or proton activity (*14, 15*). In the presence of fluids, oxygen exchange may also occur by solution reprecipitation or reaction rather than by diffusion (*8, 11, 14, 16, 17*). Thus, the removal of grain boundary fluid by retrograde reactions during the cooling of a metamorphic rock could cause sudden cessation of oxygen diffusion. These observations raise the possibility that individual mineral grains might preserve microscale information of their thermal or fluid-rock interaction histories (*7*).

Advances in the microanalysis of stable isotope ratios in minerals by the ion microprobe–secondary ion mass spectrometer have allowed researchers to decipher the isotopic record within individual mineral grains as initially demonstrated for magnetite (*7*). In well-constrained cases where zonation patterns are known, their interpretation can provide a more fundamental understanding of the thermal evolution and the fluid-rock interaction in the Earth's crust.

In this report, we describe the first detailed mapping of oxygen isotope ratios in a single mineral grain, a large magnetite crystal from a granulite facies marble from the Adirondack Highlands, New York, and discuss implications for the processes that redistribute oxygen during cooling of metamorphic rocks. The magnetite crystal is from the Weston Mine, a magnetite skarn at the contact of the Marcy anorthosite massif in the central Adirondack Highlands. These rocks have experienced a complex metamorphic history (*18, 19*) of contact metamorphism and metasomatism ($\sim$900°C, <3 kbar), regional Grenville-age (1080 to 1050 million years ago) granulite facies metamorphism at about 775°C and 7.5 kbar, and finally late-stage alteration during slow cooling, 1° to 3°C per million years (*20*). Large amounts of aqueous fluids were involved during skarn formation, small amounts of grain boundary fluids were present during

---

J. W. Valley, Department of Geology and Geophysics, University of Wisconsin, Madison, WI 53706.
C. M. Graham, Department of Geology and Geophysics, University of Edinburgh, Edinburgh EH9 3JW, Scotland, United Kingdom.

*To whom correspondence should be addressed.

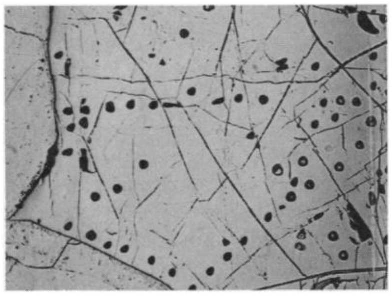

Fig. 1. Reflected light photomicrograph of the lower left quarter of sample 90LP9a before it was repolished (*24*). The full grain is shown in Fig. 2, A and B. Ion probe pits measure 35 μm in diameter by 1.5 μm deep and individual analyses of $\delta^{18}O$ came from the central 8 μm of each pit.

late alteration, and fluids were absent from these rocks at the peak of granulite facies metamorphism (*19*).

Sample 90LP9a is a granulite facies marble. We have described the geology and reported conventional and ion microprobe–oxygen isotope analyses of a mineralogically similar sample, LP204-1 (*7*). The 90LP9a sample contains magnetite (~22% by volume), calcite (58%), diopside (16%), and monticellite (4%). Late alteration minerals replaced monticellite, filling late cracks that are typically 1 to 5 μm thick in magnetites. Magnetites are up to 6 mm across, and we have made 115 ion probe analyses for $\delta^{18}O$ from one grain that measures 3 mm by 5 mm (Figs. 1 and 2). This magnetite is close to end-member Fe_3O_4 in composition (*21*), and examination by reflected light, electron microprobe analysis, backscattered electron imaging, and secondary electron microscopy indicates that it is homogeneous.

Conventional bulk-mineral analyses (*22*) (Table 1) show that the variation in $\delta^{18}O$ of the magnetites [9.6 to 10.8 per mil, standard mean ocean water (SMOW)] is significantly larger than the 0.2 per mil (1 SD) reproducibility of repeat analyses on powders. Therefore, this value represents small but real differences among the bulk compositions of individual magnetite grains (average composition, 10.35 ± 0.33 per mil; all analyses from Table 1). Laser probe analyses in Table 1 show a systematic variation of $\delta^{18}O$ with grain size, with the average composition of the largest analyzed grains (3 mm by 3.5 mm by 4.5 mm, $\delta^{18}O = 10.74$) higher than for smaller grains (average diameter, 1.1 mm; $\delta^{18}O = 10.05$). This variation (0.7 per mil) is similar to, though not as large as, the variation measured between large and small grains in a nearby sample (LP204-1, 1.2 per mil) (*7*). These variations are consistent with the hypothesis that $\delta^{18}O$ is lower in the rims of each crystal and that larger crystals have a smaller proportion of rim material.

The average $\delta^{18}O$ of six calcites from 90LP9a is 18.7 per mil, and the apparent bulk-mineral fractionation between calcite and magnetite is 8.3 per mil. If these bulk-mineral compositions represent homogeneous equilibrium values, then the apparent oxygen isotope temperature would be 570°C (*3*), which is much less than the peak granulite-facies temperature of 775°C (*18*). The bulk-material values for LP204-1 are even more reset with a fractionation of 9.3 per mil and an apparent temperature of 525°C.

We have analyzed oxygen isotope ratios in magnetite and ilmenite with the Cameca (Courbevoie, France) ims-4f ion microprobe at the University of Edinburgh (*7, 23*), and analytical procedures have been reported in detail (*7, 24*). The analytical spot size is confined to an area 8 μm in diameter by the $^{133}Cs^+$ beam (~35-μm diameter) that was used to ionize the sample and by a series of apertures and lenses that focused the secondary O^- beam during energy and mass analysis. Each pit is 1.5 μm deep for an analyzed volume of ~75 μm^3 (~390 pg); these spots are $<10^{-11}$ the weight of the 50 to 200 g pieces of rock from which magnetite was concentrated for conventional analysis (Table 1). The analysis of one spot requires about 45 min, during which time 10^6 ions of ^{18}O are counted; the 1 SD uncertainty in $\delta^{18}O$ is thus 1 per mil.

Figure 1 shows individual ion probe pits, 35 μm across, from a portion of sample 90LP9a after the first 68 analyses were completed. Figure 2A shows the entire grain (Fig. 1 is the lower left corner) with values of $\delta^{18}O$ plotted for all 115 analyses. These analyses were standardized by 47 analyses of standard magnetite that were interspersed after every five to ten sample analyses. The reproducibility of the standard data varied from 0.9 to 1.6 per mil and the uncertainty of the mean standard value varied from 0.2 to 0.6 per mil (1 SD) during

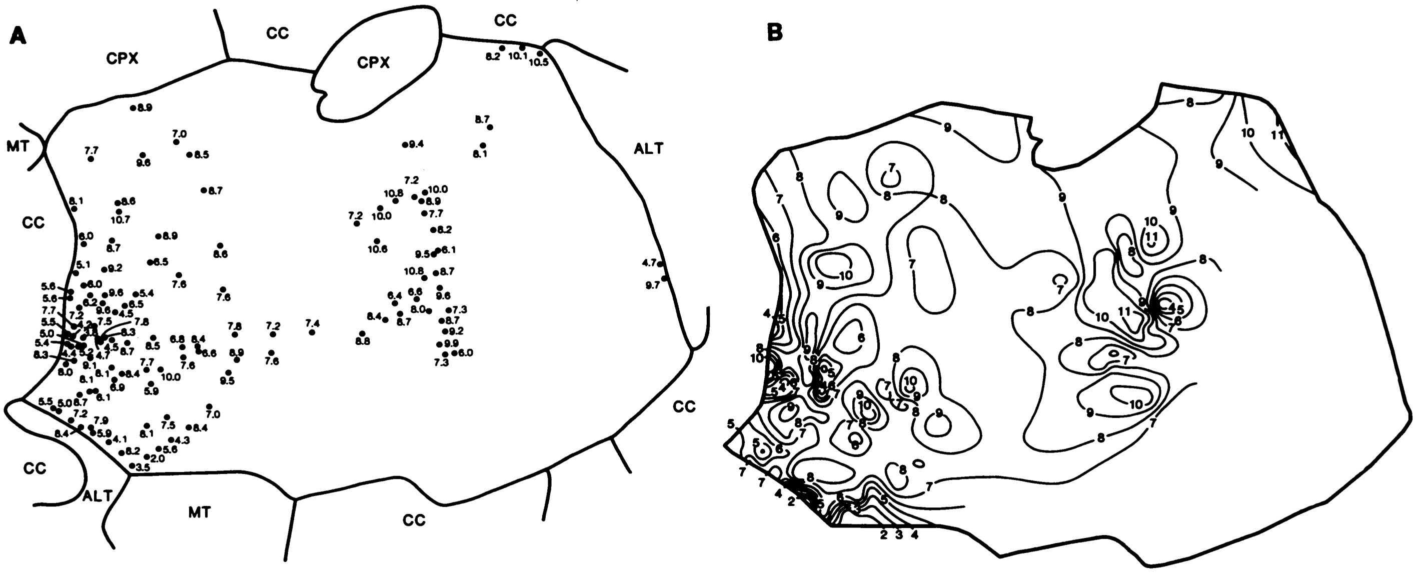

Fig. 2. (**A**) Sample 90LP9a showing the $\delta^{18}O$ SMOW values of 115 ion microprobe analyses. (**B**) Map of the oxygen isotope composition of a magnetite grain from the same sample as in (A) (3 mm by 5 mm), on the basis of 115 independent spot analyses by ion microprobe (Fig. 2A). The 1 per mil contours of $\delta^{18}O$ were made by computer (*25*) for all data points except two on the right margin. Variability of 9 per mil is recorded, and low $\delta^{18}O$ values are concentrated near the grain boundary. Maximum gradients of 2 to 4 per mil per 100 μm are up to 50 times less severe than those measured by depth profiles of smaller magnetites from this locality (9 per mil per 10 μm, LP204-1). Scale bar in lower right of (B) is 1 mm.

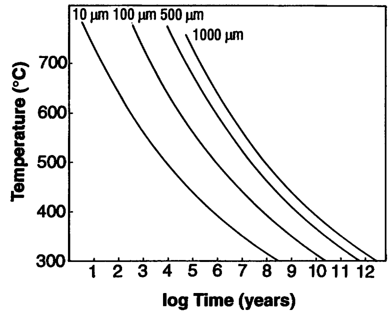

Fig. 3. Calculations of the approximate time required for oxygen to diffuse distances of 10 to 1000 µm in magnetite.

the five analytical sessions. Individual analyses are accurate and precise to within ~1 per mil (1 SD) (*24*).

We digitized the 115 corrected $\delta^{18}O$ spot analyses (Fig. 2A) together with their positions in the 90LP9a magnetite crystal and generated a contoured $\delta^{18}O$ map (*25*) (Fig. 2B). The general features shown by these contours are robust to variation of contouring parameters. Two principal features of the results are: (i) The single magnetite grain shows a wide range of $\delta^{18}O$ from +2 to +11 per mil, comparable to that measured within several magnetite grains from sample LP204-1 (0 to +11 per mil) (*7*). (ii) The highest $\delta^{18}O$ values are in the center of the 90LP9a grain and the lowest values are concentrated near the edges. However, the distribution of $\delta^{18}O$ is irregular on a scale of hundreds of micrometers. Gradients of 2 to 4 per mil per 100 µm have been measured in many areas where analyses are 160 to 375 µm apart (Fig. 2, A and B). This pattern is in stark contrast to that in LP204-1, which is homogeneous except for rims 10 µm wide that have low $\delta^{18}O$ values and steep, smooth gradients of 9 per mil over 10 µm.

Table 1. Bulk-mineral stable isotope compositions of magnetite and calcite. Magnetites were heated for reaction with BrF_5 by resistance furnace or by laser probe. Values of $\delta^{18}O$ SMOW and $\delta^{13}C$ Pee Dee belemnite standard were measured by conventional gas-source mass spectrometry.

Sample	Weight (mg)	$\delta^{18}O$ (per mil)	
Magnetite, resistance-heated Ni bombs			
90LP9a-12		10.64*	
90LP9a-12		10.17*	
90LP9a-12		10.52*	
Magnetite, laser probe			
90LP9a	2.7	10.75†	
90LP9a	2.7	10.58†	
90LP9a	3.7	10.67†	
90LP9a	3.1	10.29†	
90LP9a	2.3	10.73†	
90LP9a	3.0	10.46†	
90LP9a-1	1.7	10.83‡	
90LP9a-1	2.8	10.65‡	
90LP9a-4	1.8	10.08§	(0.9)
90LP9a-5	4.3	10.06§	(1.2)
90LP9a-6	4.4	10.13§	(1.2)
90LP9a-7	3.3	10.31§	(1.1)
90LP9a-8	2.4	9.99§	(0.9)
90LP9a-9	2.8	9.63§	(1.0)
90LP9a-10	8.1	9.87§	(1.5)
90LP9a-11	3.1	10.29§	(1.1)
90LP9a calcite		18.67‖	

*Single crystal, 4.5 mm by 5.5 mm by 5.5 mm, powdered. †Powdered grains, 1 to 2 mm in diameter. ‡Single crystal, 3 mm by 3.5 mm by 4.5 mm, powdered. §Single crystals, not powdered, diameter given in parentheses in millimeters. ‖Average of six analyses, $\delta^{18}O$ ranges from 18.28 to 18.98, $\delta^{13}C = -1.97 \pm 0.03$ (1 SD).

The smooth profiles in $\delta^{18}O$ at the edge of LP204-1 magnetite grains suggest that the mechanism of exchange was diffusion inward from the grain boundary. The simple geometry of these gradients facilitates quantitative predictions and tests of this hypothesis (*7, 10*). In contrast, the complex distribution of $\delta^{18}O$ values in 90LP9a currently precludes quantitative evaluation. However, the analysis and understanding of a sample such as 90LP9a are important because they help to explain the processes of retrogression and to establish the limits of thermometry and diffusion modeling.

The irregular $\delta^{18}O$ distribution in 90LP9a (Fig. 2B) cannot be explained by simple inter-mineral diffusive exchange of oxygen during cooling. We proposed that the low values on the rims of LP204-1 magnetites resulted from the diffusive exchange of magnetite ($\delta^{18}O$ = 9 to 11 per mil) and retrograde hydrous fluids ($\delta^{18}O$ = 7 to 8 per mil) at temperatures of 300° to 500°C (*7*). The presence of low-temperature hydrous alteration minerals in both samples demonstrates such fluid infiltration. Similar late-stage fluids were common throughout the adjacent anorthosite massif (*26*).

Evaluation of the possible explanations of these features depends, as a limiting boundary condition, on the length scale of oxygen diffusion in magnetite. If grain boundaries are held at a constant composition, C_0, such as might result from fluid infiltration, then the length scales of diffusion can be estimated from the expression for diffusion in a semi-infinite medium (*27*). In this expression, C is the concentration at distance x from the grain boundary, D is the diffusion coefficient, and t is the time of exchange. If a value of $C/C_0 = 0.1$ is assumed (that is, 90% exchange at distance x), then $x = 2.33 \sqrt{(Dt)}$ (*7, 27*) (Fig. 3).

Could isotopic heterogeneity that formed before the peak of granulite facies metamorphism be partially preserved? If so, then isotopic zonation could result from variable compositions of skarn fluids and possibly from the coalescence of several smaller crystals. However, using experimental diffusion data for oxygen in magnetite (*28*), we calculated that heterogeneities on the scale observed in 90LP9a would be smoothed out in $<10^5$ years at the temperatures of granulite facies metamorphism (Fig. 3). Even if the activity of water was low and diffusion of oxygen in magnetite was considerably slower than is indicated by the hydrous experiments (*12*), any significant heterogeneities would have been smoothed out in $<10^7$ years, a reasonable time span for granulite facies annealing. Thus, isotopic equilibrium and homogeneity prevailed in these samples at the peak of regional metamorphism.

At a peak metamorphic temperature of 775°C, the equilibrium fractionation of oxygen isotopes causes calcite to have a value of $\delta^{18}O$ that is 5.4 per mil greater than that in magnetite (*3*). This value is ~3 per mil less than the bulk-mineral fractionations measured conventionally in 90LP9a (Table 1). Mass balance and the modal proportions of 90LP9a indicate that if exchange occurred during cooling without significant fluid infiltration, then the average value of magnetite would have shifted downward ~2 per mil, from 12 to 10 per mil; calcite would have shifted upward a proportionately smaller amount. Only if fluids infiltrated these rocks at the time of exchange could the $\delta^{18}O$ of magnetite have been shifted to the low values that are seen in 90LP9a.

Thus, the pattern of $\delta^{18}O$ variation and the low values seen in Fig. 2B resulted from exchange between the magnetite and an externally derived, late-stage fluid, comparable to fluid that exchanged with magnetites in LP204-1. However, the development of an irregular pattern of oxygen exchange that occurs hundreds of micrometers from the magnetite grain boundary requires different mechanisms from those recorded in LP204-1. Regardless of the relative importance of diffusion versus recrystallization, it is clear that effective exchange distances were reduced by access of fluid directly to the interior of the 90LP9a crystal. If present, microfractures or micropores would have provided suitable fluid channels, facilitating exchange and extending low $\delta^{18}O$ domains into the crystal (*29*). The preservation of the resulting isotopic heterogeneity over time scales of millions of years is only possible at temperatures <400°C in a hydrous environment (Fig. 3).

The two samples were carefully studied for evidence that cracks or pores had facilitated oxygen isotope exchange. Both the 90LP9a magnetite grain (Fig. 1) and the LP204-1 magnetites (*7*) (Fig. 4) contain plentiful cracks, some of which are filled with later minerals. However, $\delta^{18}O$ does not correlate with position relative to these cracks, and the distribution of cracks is similar in the two rocks. Before ion probe

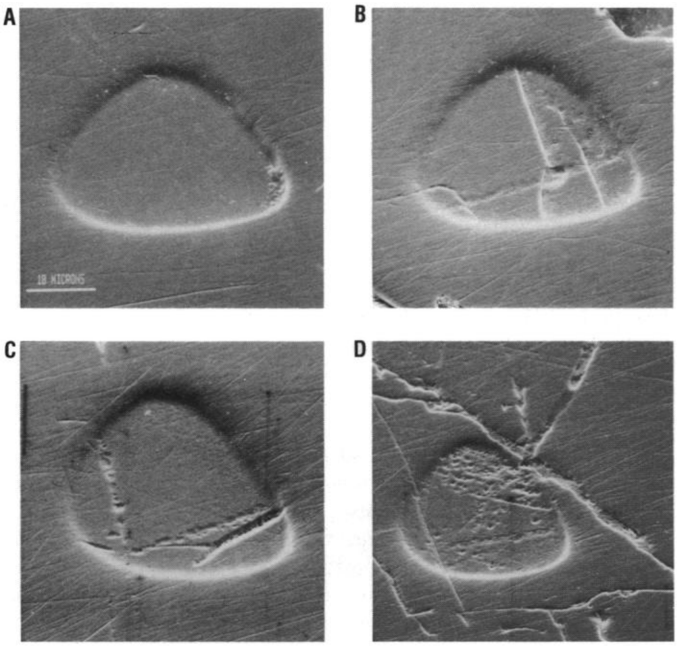

Fig. 4. Scanning electron microscope images of individual ion microprobe pits in magnetite. (**A**) A typical pit in LP204-1; (**B** to **D**) show #108, #103, and #110, respectively, in 90LP9a. Figure 4, A to C, are at the same magnification [see bar in (A)]. Most pits in LP204-1 are similar to that shown in (A), smooth and featureless; fine scratches are from polishing after analysis. In contrast, most pits in 90LP9a contain cracks and micropores. These cryptic features are often visible only where they have been preferentially eroded by the high-energy ion beam. The presence of cracks or pores would have facilitated oxygen isotope exchange in 90LP9a, causing the extreme heterogeneity, but LP204-1 was not similarly affected.

analysis, each sample was examined by scanning electron microscope (SEM) (×2000), electron microprobe analysis, backscattered electron imaging, and reflected light microscope (×240). During ion probe analysis, each spot was imaged for cracks. No differences among the two samples were evident. After analysis the ion probe pits were examined optically and by SEM.

SEM images were taken of ion probe pits in LP204-1 (Fig. 4A) and 90LP9a (Fig. 4, B to D). Over 90% of the pits in LP204-1 show smooth, featureless bottoms (Fig. 4A). In contrast, 92% of the pits in 90LP9a contain fine cracks or linear traces of micropores. In all cases, these cryptic cracks and pores appear as features that existed before the analysis and that have been accentuated by preferential erosion during analysis. Most of the features seen in Fig. 4, B to D, are not visible outside of the pit itself and could not have been seen before analysis. The cracks appear to be healed, which distinguishes them from the group of open cracks seen in Fig. 1. It is possible that the micropores seen in Fig. 4D correlate to the adjacent open crack, but the relative timing of these features is not known.

If cracks or pores were present when retrograde fluids infiltrated 90LP9a, then they would have provided conduits for rapid and heterogeneous oxygen exchange deep into the large magnetite crystal. If the larger, open cracks formed later, then LP204-1 was free of such features at the time of retrograde exchange. This timing explains why low $\delta^{18}O$ values are found only at the grain boundaries. To investigate this hypothesis, we categorized the 115 pits in 90LP9a according to the intensity of cracks. No correlation has been found yet between the intensity of cracks or pores and the measured values of $\delta^{18}O$. However, this lack of correlation may result from the small areas that have been exposed in each pit for examination. Important cracks with diffusion halos may pass near pits without being seen. Furthermore, there are several generations of these cryptic features and they may not have been equally important during retrograde exchange.

A question also remains as to why two similar samples of magnetite-bearing marble should show such differences. Retrograde processes may have been so localized that one rock was much more affected than the other. Conversely, it seems likely that the rheology of the two rocks was affected by the relative amounts of ductile calcite and by the sizes of the brittle magnetites. Thus, the magnetites 5 mm in diameter that are in 90LP9a with only 58% calcite may have been broken during late deformation, whereas the 1-mm magnetites in LP204-1 with 75% calcite were cushioned.

We conclude that oxygen exchange has occurred between retrograde fluids and 90LP9a magnetite along cryptic microfractures and pores that are now partially healed. The scale of this process is so fine and the variability is so extreme that the effects cannot be fully resolved even at the ultra-high spatial resolution that we used.

The implications of the results in this study for oxygen isotope thermometry or for cooling-rate speedometry are profound. Even an unusually detailed study of differently sized grains by bulk-mineral analysis (Table 1) gives only a hint of the shocking heterogeneity seen in 90LP9a. The complexity of the $\delta^{18}O$ pattern precludes the use of oxygen isotope compositions of 90LP9a magnetites for either thermometry or cooling-rate speedometry.

Our knowledge of micro-scale variation of oxygen isotope composition of metamorphic minerals at the scale of the individual mineral grain is limited (*7, 23, 30–32*). It is not yet clear whether the patterns of intragrain variation imposed by exchange with fluids along grain boundaries or healed along microcracks and micropores will be of widespread importance. Thus, the interpretation and modeling of conventional bulk-mineral oxygen isotopic data must be treated cautiously. On the other hand, the ability to measure intragrain isotopic variations on the scale achieved in this study provides an exciting opportunity for new levels of understanding of thermal and fluid interaction histories of slowly cooled rocks.

REFERENCES AND NOTES

1. M. Javoy, *J. Geol. Soc. London* **133**, 609 (1977).
2. J. R. O'Neil and R. N. Clayton, *Isotopic and Cosmic Chemistry* (North-Holland, Amsterdam, 1964), pp. 157–168; I. Friedman and J. R. O'Neil, *U.S. Geol. Surv. Prof. Pap.* **440-KK**, 1 (1977).
3. H. Chiba, T. Chacko, R. N. Clayton, J. R. Goldsmith, *Geochim. Cosmochim. Acta* **53**, 2985 (1989).
4. J. W. Valley, H. P. Taylor, J. R. O'Neil, Eds., *Stable Isotopes in High Temperature Processes*, vol. 16 of *Reviews in Mineralogy* (Mineralogical Society of America, Washington, DC, 1986).
5. Y. Bottinga and M. Javoy, *Rev. Geophys. Space Phys.* **13**, 401 (1975).
6. P. Deines, *Geochim. Cosmochim. Acta* **41**, 1709 (1977).
7. J. W. Valley and C. M. Graham, *Contrib. Mineral. Petrol.* **109**, 38 (1991).
8. B. J. Giletti, *Chem. Geol.* **53**, 197 (1985).
9. ______, *Earth Planet. Sci. Lett.* **77**, 218 (1986).
10. J. M. Eiler, L. P. Baumgartner, J. W. Valley, *Contrib. Mineral. Petrol.* **112**, 543 (1992).
11. D. R. Cole and H. Ohmoto, in (*4*), pp. 41–90.
12. Z. D. Sharp, *Geology* **19**, 653 (1991).
13. M. H. Dodson, *Contrib. Mineral. Petrol.* **40**, 259 (1973).
14. C. M. Graham and S. C. Elphick, in *Diffusion, Atomic Ordering, and Mass Transport*, J. Ganguly, Ed. (Springer, New York, 1991), pp. 248–285.
15. B. J. Giletti and R. A. Yund, *J. Geophys. Res.* **89**, 4039 (1984); S. C. Elphick and C. M. Graham, *Nature* **335**, 343 (1988); J. R. Farver and R. A. Yund, *Geochim. Cosmochim. Acta.* **54**, 2953 (1990).
16. R. T. Gregory, R. E. Criss, H. P. Taylor, Jr., *Chem. Geol.* **75**, 1 (1989).
17. S. C. Elphick, C. M. Graham, F. D. L. Walker, M. B. Holness, *Mineral. Mag.* **55**, 347 (1991).
18. S. R. Bohlen, J. W. Valley, E. J. Essene, *J. Petrol.* **26**, 971 (1985).
19. J. W. Valley, S. R. Bohlen, E. J. Essene, W. Lamb, *ibid.* **31**, 555 (1990).
20. J. McLelland and J. Chiarenzelli, *J. Geol.* **98**, 19 (1990); K. Mezger, C. Rawnsley, S. R. Bohlen, G. Hansen, *ibid.*, p. 415.
21. The chemical composition of magnetites in sample 90LP9a is homogeneous and similar to that of LP204-1 (*7*), with (by weight) 0.65% Al_2O_3, 4.39% MnO, and 1.23% MgO. A complete set of

data is available from J.W.V.

22. Conventional oxygen isotope analyses were made of 10-mg mineral separates concentrated from a cube, 4 cm on a side (sample 90LP9a) cut from the larger block. Ion microprobe analyses were made on a thin section 2.5 cm in diameter that was cut along one face of the cube. Small pieces of calcite were removed from each of the corners of the cube; the remainder was dissolved in dilute HCl. Magnetites were then handpicked from the residue. Calcites were analyzed by conventional reaction with concentrated (density = 1.92) phosphoric acid. One large magnetite grain was powdered and analyzed by reaction with BrF_5 in conventional nickel reaction vessels that were externally heated by electric resistance furnaces. Other magnetites were reacted with BrF_5, either as powder or as intact single crystals, with a CO_2-laser heat source (*33*). The conventional and laser analyses yield similar accuracy and precision (Table 1), but the laser permits significantly smaller sample sizes.
23. J. W. Valley and C. M. Graham, *Eos* **72**, 292 (1991).
24. Analytical procedures for the analysis of oxygen isotope ratios by ion microprobe in this study followed closely the methods reported in detail by Valley and Graham (*7*). Before it was polished, a well-characterized magnetite standard (LP204-1), previously shown to be isotopically and chemically homogeneous (*7*), was epoxied into a 2-mm hole in the thin section next to the magnetite grain to be analyzed. The accuracy of these analyses is comparable to the precision on a single spot, as shown by replicate analyses of the standard: 15 analyses of LP204-1 on 5 to 6 July 1992 yielded a mean $\delta^{18}O$ of 8.9 ± 0.2 per mil (1 SD about the mean; complete set of data available from J.W.V.). During this study, after analysis 68, the standard magnetite grain was replaced and the sample was lightly ground and repolished. A layer ~10 μm thick was ground from the face of the sample at this time, which removed old analysis pits and permitted reanalysis. Figure 1 shows a portion of the sample in reflected light before repolishing. Unpublished Fig. A-1 (available from J.W.V.) shows the location of all analyzed spots. Dead-time corrected $^{18}O/^{16}O$ ratios were converted to $\delta^{18}O$ values by comparison with the LP204-1 magnetite standard. Values are reported in standard per mil notation relative to SMOW. We measured values of instrumental mass fractionation, ranging from −8 to −15 per mil, using electron multipliers that were installed in December 1990 and May 1991. These values are smaller than those previously obtained by us (*7, 22*) or by Hervig and colleagues (*34*) with a Cameca ims-3f. However, as with our earlier results, the fractionation increased with each successive day of analysis. This result supports our suggestion that when a new electron multiplier is used, instrumental mass fractionations are partly controlled by factors that relate to the aging of the detector. The chemical composition of magnetite standard LP204-1 is close to that of 90LP9a. Therefore, no additional correction for instrumental mass fractionation is necessary. Analysis of the 90LP9a sample was stopped on three occasions (after spots 68, 79, and 118) when significant drift was detected in the standard analyses. This was remedied either by adjustment to the Cs gun or by realignment. Thus, no drift corrections to the data of this study are necessary.
25. Computer-drawn contours were made with a least-squares gridding and contouring program, *Zycor Z-map Plus*.
26. J. Morrison and J. W. Valley, *J. Geol.* **99**, 559 (1991).
27. In the equation $C = C_0 \operatorname{erfc} [x/2\sqrt{(Dt)}]$, where erfc is the inverse error function, C and C_0 are concentrations normalized as a percentage of the total gradient [J. Crank, *The Mathematics of Diffusion* (Oxford Univ. Press, New York, ed. 2, 1975)].
28. B. J. Giletti and K. C. Hess, *Earth Planet. Sci. Lett.* **89**, 115 (1988).
29. F. D. L. Walker, *Contrib. Mineral. Petrol.* **106**, 124 (1990); (*17*).
30. H. Wada, *Nature* **331**, 61 (1988); Y. Arita and H. Wada, *Geochem. J.* **24**, 173 (1990); C. P. Chamberlain and M. E. Conrad, *Science* **254**, 403 (1991); M. E. Conrad and C. P. Chamberlain, *Geology* **20**, 812 (1992).
31. D. Elsenheimer and J. W. Valley, *Chem. Geol. Isotope Geosci.* **101**, 21 (1992).
32. ———, *Geol. Soc. Am. Abstr. Programs* **24**, A251 (1992); M. Kohn, J. W. Valley, D. Elsenheimer, M. Spicuzza, *ibid.*, p. 251; Z. D. Sharp, E. J. Essene, J. R. Smyth, *Contrib. Mineral. Petrol.* **112**, 358 (1992).
33. Z. D. Sharp, *Geochim. Cosmochim. Acta* **54**, 1353 (1990); D. E. Crowe, J. W. Valley, K. L. Baker, *ibid.*, p. 2075; (*31*).
34. R. L. Hervig, P. Williams, R. M. Thomas, S. N. Schauer, I. Steele, *Int. J. Mass Spectrom. Ion Processes* **120**, 45 (1992).

35. We thank J. Craven and R. Hinton for their assistance, training, and advice; M. Spicuzza, D. Elsenheimer, J. Eiler, and K. Baker for aid with conventional and laser analyses; K. Thomson and C. Kay for help with data digitizing and contouring using the seismic workstation at the University of Edinburgh; and R. Noll and N. Lawrence for help with SEM. Craven, Eiler, and two anonymous reviewers provided helpful comments. This research was initiated while J.W.V. was a Fulbright Fellow at the University of Edinburgh. Additional support came from the National Science Foundation (EAR89-05101 and 91-05709). The Edinburgh Ion Microprobe Lab is supported by the Natural Environment Research Council.

13 October 1992; accepted 15 January 1993

The $^{18}O/^{16}O$ Ratio of 2-Billion-Year-Old Seawater Inferred from Ancient Oceanic Crust

C. Holmden and K. Muehlenbachs

An oxygen isotope profile of the 2-billion-year-old Purtuniq ophiolite overlaps with similar profiles of younger ophiolites and the modern oceanic crust. This overlap implies (i) that there was a similar style of seawater–ocean crust interaction during the past 2 billion years; (ii) that the oxygen isotope composition of early Proterozoic seawater was similar to the modern value; (iii) that early Proterozoic sea-floor spreading rates were similar to, or greater than, average modern rates; and (iv) that early Proterozoic carbonate rocks and cherts with low $^{18}O/^{16}O$ ratios do not reflect global-scale ^{18}O depletion of early Proterozoic oceans.

A long-standing controversy concerns temporal variations in the oxygen isotope composition of Precambrian seawater. It has been suggested that the $\delta^{18}O$ (*1*) record of carbonates (*2–4*) and cherts (*5*) over the past 2 billion years reflects variations in the isotopic composition of the seawater in which these sediments were formed. Others argue that pervasive ^{18}O exchange between seawater and the oceanic crust caused the $\delta^{18}O$ value of seawater to remain constant over time (*6, 7*). Satisfactory resolution of such conflicting views is important in that the oxygen isotope composition of Precambrian seawater bears on the nature of Precambrian plate tectonics and climate.

In this report we show that the imprint of early Proterozoic seawater is preserved in the $\delta^{18}O$ profile of the 1.998-billion-year-old Purtuniq ophiolite, situated in the Cape Smith Belt of northern Quebec, Canada (*8–10*). The controversy surrounding the true $\delta^{18}O$ value of early Proterozoic seawater is addressed through a comparison of the isotopic imprint of 2-billion-year-old seawater determined for the ophiolite with that in contemporaneous carbonate rocks of the ~1.9-billion-year-old Rocknest dolostone, situated in the Wopmay orogen, Northwest Territories, Canada (*3, 4*). The opportunity to analyze samples from the lower levels of early Proterozoic oceanic crust distinguishes this work from most earlier studies that have utilized less desirable submarine pillow basalts collected from Precambrian greenstone terranes (*11, 12*).

From their studies of the Rocknest dolostone, Burdett *et al.* (*3*) and Veizer *et al.* (*4*) concluded that the $\delta^{18}O$ value of early Proterozoic calcite was nearly 10 per mil lower than that of modern marine calcites, which are ~30 per mil (relative to SMOW). On the basis of the excellent preservation of original marine fabrics observed in thin section, Burdett *et al.* argued that dolomitization of the primary carbonates did not completely overprint the original seawater signature. Using the isotopic composition of the most ^{13}C- and ^{18}O-enriched dolomitized ooid of 22.9 per mil and an assumed dolomite-calcite fractionation of +4 per mil, Burdett *et al.* calculated a $\delta^{18}O$ value of 18.9 per mil for the original Rocknest calcite. If equatorial seawater temperatures in the early Proterozoic were similar to today's, Burdett *et al.* (*3*) suggested, as have others (*4, 5*), that lower $\delta^{18}O$ values for early Proterozoic sediments may reflect a nearly 10 per mil ^{18}O depletion in early Proterozoic seawater.

Although widely accepted, the above proposal conflicts with predictions that the average $\delta^{18}O$ value of the global ocean

---

Department of Geology, University of Alberta, Edmonton, Alberta, Canada T6G 2E3.